

Recent Advances on Quantum-Dot-Enhanced Liquid-Crystal Displays

Haiwei Chen, Juan He, and Shin-Tson Wu, *Fellow, IEEE*

(Invited Paper)

Abstract—We review recent advances in quantum dot (QD)-enhanced liquid crystal displays (LCDs), including material formulation, device configuration, and system integration. For the LCD system, we first compare the color gamut difference between the commonly used Gaussian fitting method and that using real emission spectra. Next, we investigate the Helmholtz–Kohlrausch effect. Our simulation results indicate that QD-enhanced LCD appears 1.26X more efficient than organic light-emitting diode (OLED) display due to its wider color gamut. Finally, two new trends for QD-LCDs are discussed: 1) replacing conventional color filters with a QD array, and 2) emerging quantum rod (QR)-enhanced backlight. Their inherent advantages, technical challenges, and potential solutions are presented. We believe the prime time for QD-enhanced LCDs is around the corner.

Index Terms—Color gamut, Quantum dot (QD), Quantum rod (QR), liquid crystal display (LCD).

I. INTRODUCTION

BACKLIGHT is a critical part of liquid crystal displays (LCDs), as it affects the color gamut, optical efficiency, dynamic range, and viewing angle [1]–[4]. Presently, phosphor-converted white light-emitting diode (1pc-WLED) is the main backlight approach due to its high efficiency, long lifetime, low cost, and simple optical configuration [5], [6]. However, its broad yellow spectrum generated by the YAG:Ce³⁺ phosphor leads to a relatively narrow (75%) color gamut, which falls short of the ever-growing demand for vivid colors. In the past two decades, the color gamut evaluation metric has gradually advanced from sRGB to NTSC, and now to Rec. 2020 standard, whose coverage area in color space is nearly twice wider than that of sRGB [7]–[9]. As a result, advanced backlight technology is in high demand.

Using discrete RGB LEDs is an effective way to expand the color gamut [5], [10]–[13], except its driving circuit complexity increases [14], [15], and moreover, the high efficiency green LED is still not available [16]. Another choice to widen color gamut is to use two phosphor-converted WLED (2pc-WLED). The advantages of this approach include long term stability,

high efficiency, and low cost [17]–[20]. However, the narrowest full width at half maximum (FWHM) of the green phosphor (β -sialon:Eu²⁺) is still as broad as 55 nm [20]–[22]. While for red phosphor (K₂SiF₆:Mn⁴⁺) with five emission peaks, its individual FWHM is indeed quite narrow, but the average peak wavelength centers at \sim 625 nm, which is not deep enough [23]–[25]. As a result, the RGB lights still show a relatively large overlap after passing through the color filters. These crosstalks greatly reduce the color gamut.

Recently, quantum dot (QD)-enhanced backlight is emerging and it has found widespread applications because of following outstanding features: 1) its central emission wavelength can be tuned by controlling the size of the nanoparticles, 2) its FWHM is around 20–30 nm, which is mainly determined by the size uniformity, 3) its photoluminescence efficiency is high, and 4) its device configuration is simple [26]–[34]. Briefly speaking, the QD backlight uses a blue LED to excite green/red colloidal nanoparticles, generating a white light with three well-separated RGB peaks. Therefore, three highly saturated primary colors could be obtained, leading to splendid image quality [31], [33]. Several display manufacturers (e.g. Samsung, LG, Sony, TCL, etc.) have been adopting this promising technology. Sustainable efforts from both academic and industry would undoubtedly pave the way for QD-LCD's great success in the near future.

In this review paper, we present recent advances of QD-LCDs from material formulation [Section II] to device configuration [Section III]. In Section IV, we discuss the display system's performance, including color gamut and optical efficiency. An entoptic phenomenon called Helmholtz–Kohlrausch (H–K) effect will be studied in detail. Finally in Section V, two new trends for QD-LCDs will be highlighted: 1) replacing conventional color filters with a QD array, and 2) emerging quantum rod (QR)-enhanced backlight.

II. MATERIAL SYNTHESIS AND CHARACTERIZATIONS

Since the discovery in the 1980s, colloidal QDs have been explored extensively for various applications [35]–[40]. In general, they are nanometer sized (e.g. 2 \sim 10 nm) semiconductor particles, which are mainly governed by the quantum confinement effects. Unlike bulk material, these semiconductor nanoparticles exhibit unique optical and electrical properties dictated by their size, shape, and the quantum physics that arises at the nanoscale [28], [29], [41].

Manuscript received November 21, 2016; accepted January 3, 2017. This work was supported in part by the a.u.Vista, Inc. and in part by the AFOSR under contract FA9550-14-1-0279.

The authors are with the College of Optics and Photonics, University of Central Florida, Orlando, FL 32816 USA.

Color versions of one or more of the figures in this paper are available online at <http://ieeexplore.ieee.org>.

Digital Object Identifier 10.1109/JSTQE.2017.2649466

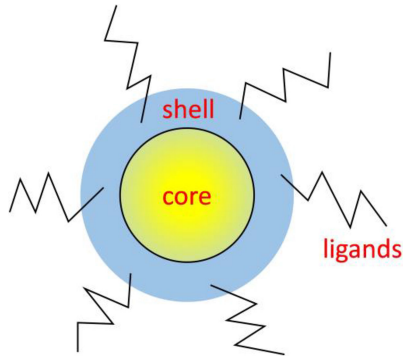


Fig. 1. Schematic diagram of QD's core-shell structure.

Briefly speaking, their desirable features can be summarized into three aspects: 1) large freedom for tailoring emission peaks. As Brus equation suggests [42]:

$$E^* \cong E_g + \frac{\hbar\pi^2}{2R^2} \left[\frac{1}{m_e} + \frac{1}{m_h} \right], \quad (1)$$

where E_g is the bandgap of bulk semiconductor, R is the particle radius, and m_e and m_h are the effective mass of electron and hole, respectively, the effective bandgap (and hence the fluorescent light) of a QD system is dependent on the particle size. For example, a 2-nm diameter CdSe QD would emit blue light, while an 8-nm CdSe QD would emit in deep red. In principle, we can get any color in the visible region by simply controlling the particle size during the synthesis process. 2) High purity emission colors. Through the sophisticated chemical synthesis techniques, QD's particle size can be controlled precisely and uniformly [30]. The corresponding FWHM of Cd-based QDs is ~ 30 nm. It is believed that 25-nm FWHM QDs in green and red could be commercially available in the next few years [28]. With some modifications, 10-nm FWHM colloidal particles have been reported in the form of platelets [43], [44]. Such a narrow emission linewidth would undoubtedly produce an exceedingly wide color gamut. 3) Excellent quantum yield and stability. This is attributed to the unique core-shell structure of QDs, as Fig. 1 shows [37], [38]. Shells as well as the surrounding organic ligands work as the protection layer and provide necessary processability. Both efficiency and lifetime would be enhanced compared to the core-only systems [45]–[47].

Various QD materials have been synthesized and studied [37], [38], [48]–[51]; they can be roughly divided into two groups: heavy metal-based QDs and heavy-metal-free QDs. Here, we choose CdSe and InP as representatives from each group for discussing their characteristics.

A. Heavy Metal-Based QDs

II-VI semiconductor CdSe is the most developed and well characterized QD material system [37], [38]. Its bulk bandgap is 1.73 eV ($\lambda = 716$ nm). According to Eq. (1), its emission spectrum can be adjusted to cover the entire visible region by tailoring the particle size, as illustrated in Fig. 2(a) [36], [52]. Meanwhile, with the mature hot-injection technique described by Bawendi and co-workers [36]–[38], Cd-based QDs exhibit quite narrow FWHM (20 \sim 30 nm) and super high luminescent

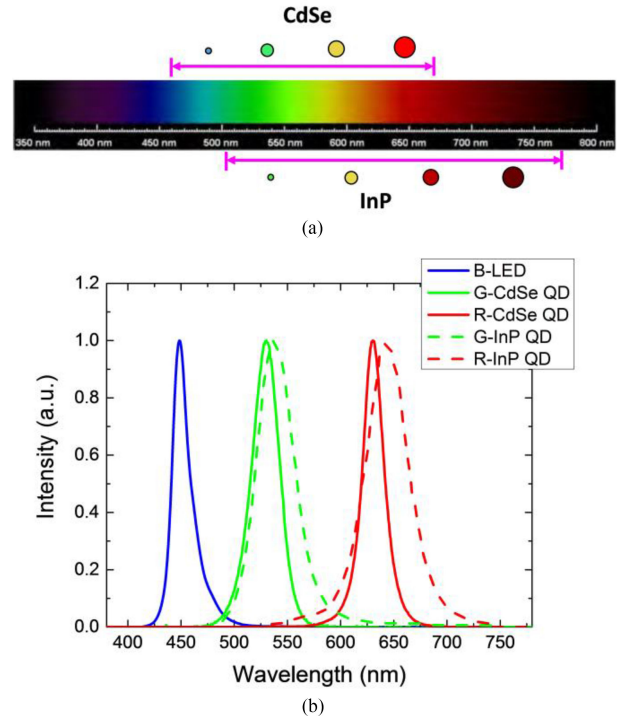


Fig. 2. (a) Potential emission spectral range of CdSe and InP QDs; (b) Typical emission spectra for green and red quantum dots using CdSe (solid line) and InP (dashed line). Blue LED with emission peak $\lambda = 450$ nm is also shown here.

quantum efficiency ($>95\%$). Fig. 2(b) depicts the typical emission spectra for green and red CdSe QDs as well as a high power InGaN blue LED. With commercially available color filters, 90% Rec. 2020 color gamut has been realized [33], [53], [54]. Such a high quality QD material seems to be a perfect choice for display applications. Indeed, Cd-based QDs have already been employed in some commercial products. However, owing to its toxicity, there is increasing demand for manufacturers to eliminate cadmium, along with other heavy metals, from consumer products. For example, in 2003 the European Union issued a directive known as the Restriction of Hazardous Substances (RoHS) [55], where the maximum cadmium content is limited to 100 ppm in any consumer electronic product. Therefore, heavy metal-free or low Cd content QDs become the new trends for future display applications [56].

B. Heavy Metal-Free QDs

Among several candidates for Cd-free QDs, InP has been identified as the most viable alternative for the visible light [48], [49], [57]–[60]. Its bandgap for bulk material is 1.35 eV, which is smaller than that of CdSe. Thus, to reach the same emission wavelength, the core size of InP dots has to be smaller than that of CdSe [Fig. 2(a)]. Smaller bandgap and smaller particle size lead to much stronger confinement effect. Thus, the emission spectrum of InP QDs is more susceptible to particle size variation [48]. As a result, its FWHM is somewhat broader (>40 nm), as shown in Fig. 2(b), corresponding to 70–80% Rec. 2020 color gamut, depending on the color filters employed. What's more, its quantum yield and stability are slightly inferior

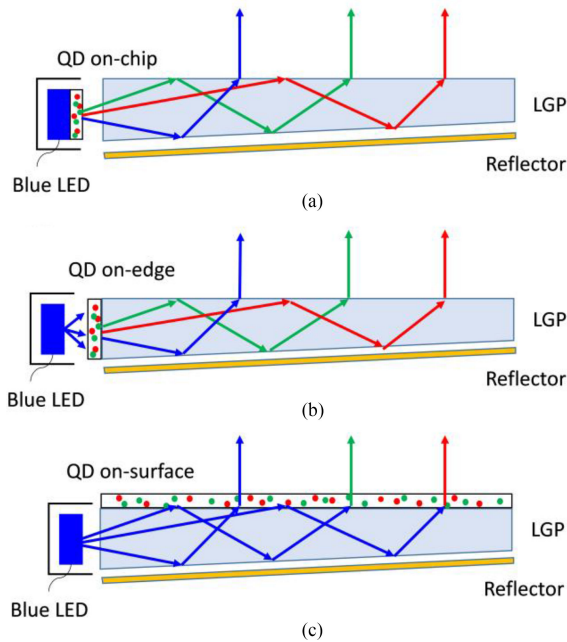


Fig. 3. Schematic diagram for three different device geometries implementing QD mixtures. (a) QD is placed within an LED package. (b) QD is placed between LED and light guide plate, or known as quantum rail. (c) QD is placed on the top surface of light guide plate, or known as quantum dot enhancement film (QDEF). (LGP: light guide plate).

to those of Cd-based QDs, mostly due to the immature chemical synthesis method [56], [61]–[64]. In 2015, Nanoco claimed to have improved the InP lifetime to over 30,000 hours using their “molecular seeding” synthesis method [63]. Once their FWHM can be further reduced, InP QDs will be more attractive for display applications. As a matter of fact, such a Cd-free backlight has already been widely used in Samsung’s TV products, and it exhibits excellent performances including wide color gamut and long lifetime [65].

Another thing worth mentioning here is, to be compliant to RoHS regulations, Nanosys proposed a “greener” QD system by combining the Cd-free and low Cd-based QDs [64]. This hybrid approach not only retains 90% Rec. 2020 color gamut but also complies with the RoHS regulation.

So far, RoHS sets the upper limit for heavy metal-based QDs. Although InP is not currently on the list, it could be reevaluated in the future. As a result, other environmentally friendly QD materials need to be developed.

III. DEVICE CONFIGURATIONS

Three QD backlight geometries have been commonly used [28]: they are “on-chip”, “on-edge” and “on-surface”, as Fig. 3 depicts. Each design has its own pros and cons, and should be chosen carefully based on different applications.

A. On-Chip Geometry

This design consumes the least amount of QD material, and is cost effective. Also, it is fully compatible to current backlight unit, leading to much simpler optical design [26], [66]. What we need is to simply replace the phosphors with QD mixtures as the energy down-conversion layer, within an LED package,

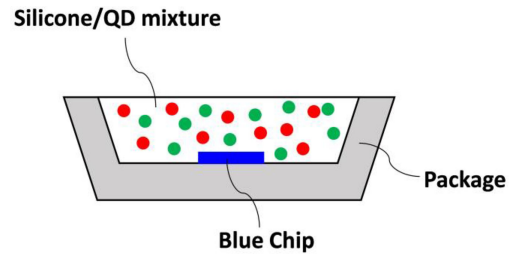


Fig. 4. Schematic diagram of QD on-chip geometry.

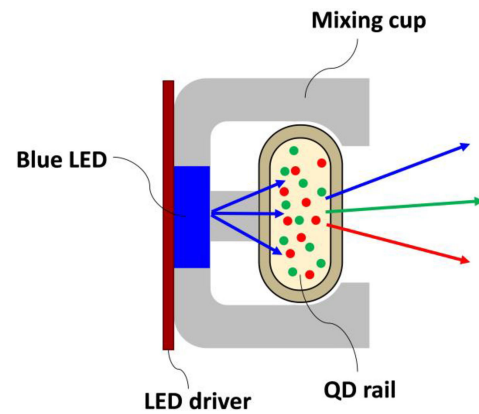


Fig. 5. Schematic diagram of QD on-edge geometry (i.e. QD rail).

as shown in Fig. 4(a). However, due to the high flux and high LED junction temperature ($\sim 150^\circ\text{C}$), the lifetime and stability of QDs could be sacrificed significantly [33], [67]. Another concern is the packaging issue, as QDs are highly sensitive to water vapor and oxygen. Hermetic sealing is necessary, which in turn increases the total cost and design complexity [28]. Nevertheless, some progress has been achieved. As reported by Pacific Lighting in 2014 [66], their on-chip testing results of QDs show no clear degradations within 3000 hours under a flux condition of 52 W/cm^2 at 85°C and 85% relative humidity. Similar results were reported by Sun *et al.* in 2016 [68].

B. On-Edge Geometry

Because the on-chip design is not yet mature for practical display applications, the on-edge geometry becomes a suitable alternative, especially for large size TVs [33]. In fact, Sony released its 55” QD TV using such configuration in 2013 [69]. Compared to on-chip design, QD rail’s lifetime is much improved because it is located further away from the blue LED. Also, the consumption of QD material is still acceptable. However, assembly is a potential issue, as Fig. 5 depicts. QD rail is first mounted into a mixing cup, and then sandwiched between the blue LED bar and the light guide plate (LGP) [70]. Here, the mixing cup is a mechanical structure, typically molded from a highly reflective plastic. It can hold the QD rail as a bracket, while directing the emitted light towards the LGP. For such a configuration, both optical efficiency and color uniformity should be considered together. Detailed discussions for the opto-mechanical optimizations have been reported in [70]. Briefly speaking, there exists an inherent trade-off between efficiency and color uniformity, so that several parameters need

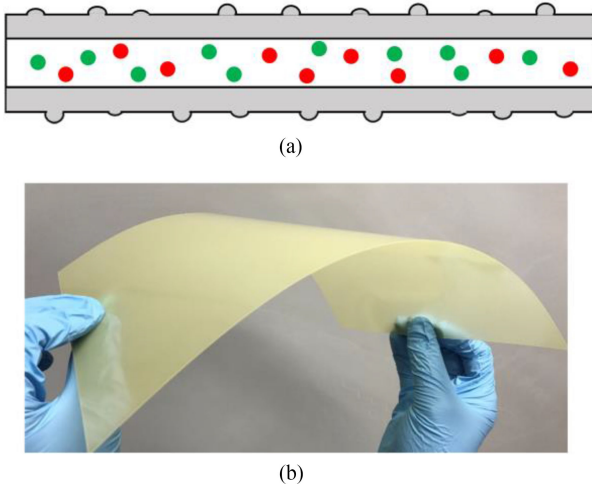


Fig. 6. (a) Schematic diagram and (b) photographic image of QD on-surface geometry (i.e. QDEF).

to be carefully designed, like scattering particles concentration in QD matrix, distance between QD rail and LGP, QD rail's size, etc.

C. On-Surface Geometry

This is the most commonly used geometry, also known as quantum dot enhancement film (QDEF) [71]. It is placed above the LGP [Fig. 3(c)], decoupled from the LED heat source spatially. As a result, the resultant operating temperature should be close to the room temperature. Both reliability and long-term stability are enhanced significantly. In fact, a lifetime over 30,000 hours has been achieved by the accelerated aging experiments [72]. Fig. 6(a) shows a sketched structure of QDEF, which comprises three layers – two plastic barrier films sandwiching a layer of quantum dots suspended in a polymer matrix [73], [74]. The barrier film for QDEF is optically clear to let light pass through, flexible for rolling and thin to allow a slim device profile, while prevents degradation from oxygen and moisture in a package. QD layer contains trillions of red- and green-emitting quantum dots, yielding yellow appearance for QDEF, as shown in Fig. 6(b). One drawback of QDEF is the massive material consumption, especially for large screen TVs. As the capacity of QDEF keeps growing, the cost should decrease gradually in the near future.

IV. SYSTEM PERFORMANCE

After introducing QD materials formulation and device configuration, next let us analyze the optical performance of an LCD system [27], [31]. Fig. 7 shows the system configuration of a typical LCD panel [75]. The incident light $S_{in}(\lambda)$ is split into three channels: red (R), green (G) and blue (B) corresponding to RGB color filters. Then they pass through the thin film transistor (TFT) backplane, LC layer, and color filter array successively. Finally, the RGB channels mix together and transmit out of the LCD panel with spectrum given as:

$$S_{out}(\lambda) = S_{out,R}(\lambda) + S_{out,G}(\lambda) + S_{out,B}(\lambda). \quad (2)$$

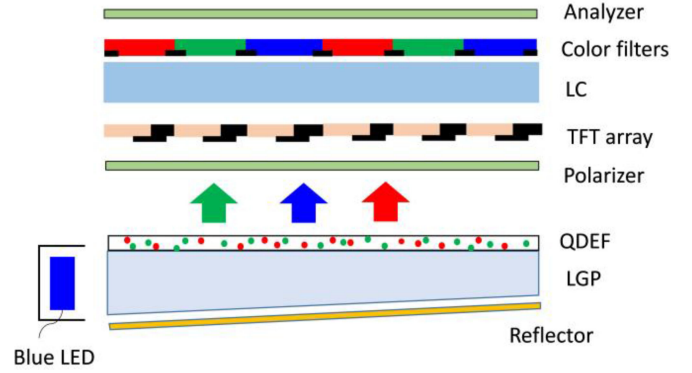


Fig. 7. System configuration of a typical LCD panel. (LC: liquid crystal; TFT: thin-film transistor).

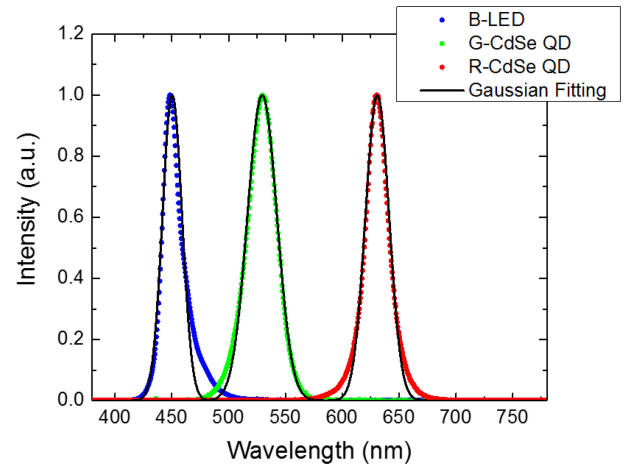


Fig. 8. Gaussian fitting of the white light spectrum using a blue LED to excite green/red CdSe QDs.

As usual, two metrics are defined here to evaluate the back-light performance: total light efficiency (TLE) and color gamut.

$$TLE = \frac{683 \frac{lm}{W} \int S_{out}(\lambda) V(\lambda) d\lambda}{\int S_{in}(\lambda) d\lambda}. \quad (3)$$

TLE represents how much input light transmits through the LCD panel and finally gets converted to the brightness perceived by the human eye. Here, $V(\lambda)$ stands for the human eye sensitivity function [76]. Unless otherwise stated, all the TLE s presented here are evaluated at the same white point D65.

As for color gamut, three color coordinates could be calculated using the output spectrum for each channel, i.e. $S_{out,R}(\lambda)$, $S_{out,G}(\lambda)$, and $S_{out,B}(\lambda)$. Then the triangular area defined by the color coordinates of the RGB primaries (the color gamut of the system) is compared to the standard gamut, like NTSC or Rec. 2020. The color gamut of the system can then be described as a percent coverage or percent area for a gamut [54].

A. Gaussian Fitting Effect

As shown in Fig. 2(b), QD emission spectrum is Gaussian-like, and so is blue LED. Thus Gaussian fitting is commonly conducted to extract the peak wavelength and FWHM [Fig. 8]. To make it simple, in some cases, the fitted curves are employed

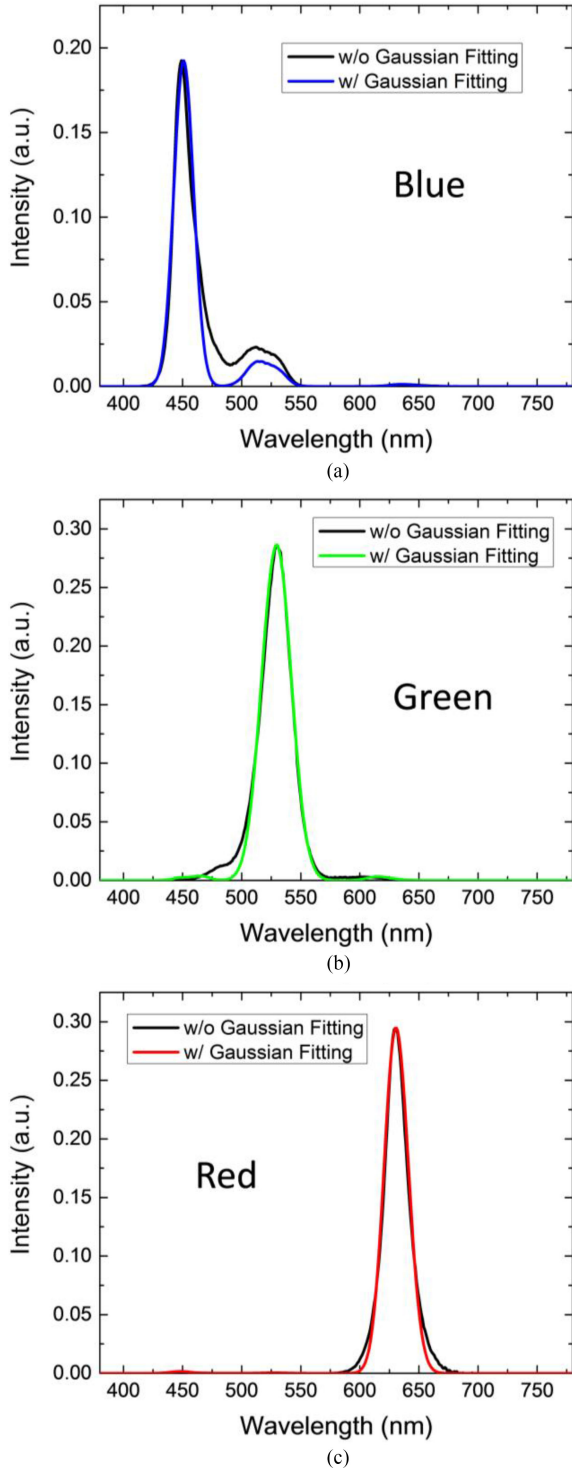


Fig. 9. (a)-(c) Calculated output spectra for blue, green and red primary colors after LC layer and color filters (CF-1).

directly into further calculations and optimizations for color gamut and other metrics by neglecting the fitting discrepancy [27], [31], [54]. Here, we discuss this Gaussian fitting effect and investigate how much it influences the final color performance.

Let us use blue LED and green and red CdSe QDs, as Fig. 8 depicts, as examples. The fitted peak wavelengths for three primary colors are $\lambda_B = 450.4$ nm, $\lambda_G =$

TABLE I
CALCULATED COLOR GAMUT AND TOTAL LIGHT EFFICIENCY
FOR SPECTRUM WITH AND WITHOUT GAUSSIAN FITTING

	Rec. 2020		TLE (lm/W)
	CIE 1931	CIE 1976	
w/ Gaussian Fitting	87.7%	88.1%	26.2
w/o Gaussian Fitting	82.4%	76.2%	28.0

529.5 nm, and $\lambda_R = 630.8$ nm. The corresponding FWHM is $\Delta\lambda_B = 20.3$ nm, $\Delta\lambda_G = 30.5$ nm, and $\Delta\lambda_R = 24.4$ nm by Gaussian fittings. Clearly, some discrepancies in the tails are observed, especially for blue LED. For R/G QDs, there exists longer emission tails than Gaussian function could predict. Such problem is more noticeable for the InP QDs, as shown in Fig. 2(b). During our calculations, commercial color filters (CF-1) are employed [27], whose transmission spectra will be shown later.

Fig. 9 shows the calculated output spectrum for each primary color after LC layer and CF-1. As expected, the spectra with Gaussian fitting exhibit much weaker color crosstalk; less light leakage results from the emission tails. Whereas for real spectrum without Gaussian fitting, there is a noticeable bump in the blue and green regions, which would deteriorate the color purity and shrink the color gamut.

The color gamut shrinkage can be visualized more clearly in Fig. 10. In both color spaces, CIE 1931 and CIE 1976, green and blue coordinates with Gaussian fitting expand outwards, leading to a much wider color gamut than that of real spectrum. The simulated results are listed in Table I. In CIE 1931, the color gamut with Gaussian fittings is 5.3% wider than that using the real spectrum. While in CIE 1976, this difference is increased to 11.9%. This discrepancy is too large to be neglected. Therefore, we should use the real spectrum instead of using fitted curves when carrying out future calculations. It is worth mentioning here: due to the light leakage shown in Fig. 9, continuing to decrease the FWHM of QDs, e.g. from 30 nm to 20 nm and then to 10 nm, will not improve the color gamut noticeably. Rather, it will eventually lead to a saturated color gamut.

B. Color Filter Effect

Besides backlight, color filters also play an important role in determining LCD's color performance. Fig. 11 shows the transmission spectra of two commercial color filters: CF-1 has higher transmittance but larger overlap between blue/green and green/red regions, while CF-2 has less color crosstalk, but the transmittance is lower, especially in the blue and green regions.

Fig. 12 shows the calculated color gamut and light efficiency. For comparison purpose, besides CdSe and InP QDs, we also include three other light sources: 1) cold cathode fluorescent lamp (CCFL), 2) yellow phosphor-converted white LED (1pc-WLED), and 3) green and red phosphor-converted white LED (2pc-WLED). Their emission spectra are obtained from [20] and [77]. Moreover, an OLED is also included here for comparison

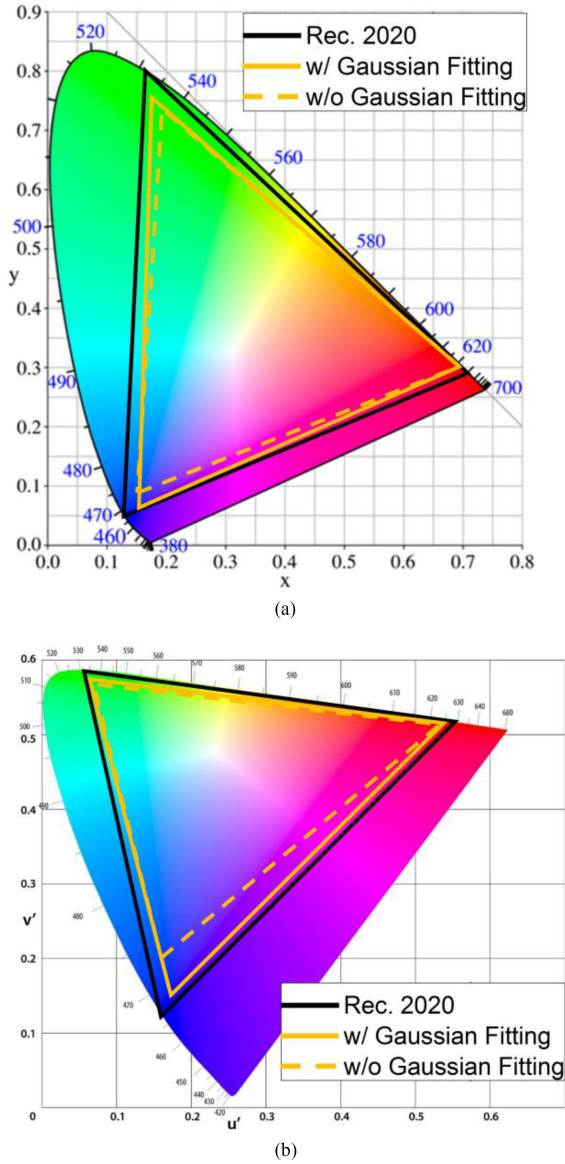


Fig. 10. Simulated color gamut in (a) CIE 1931 and (b) CIE 1976 color space.

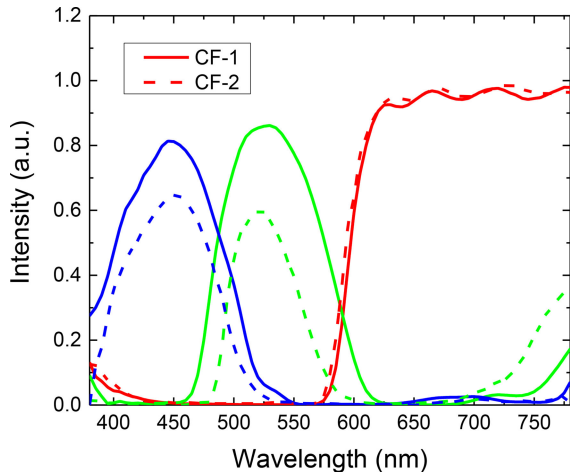


Fig. 11. Transmission spectra of two commercial color filters.

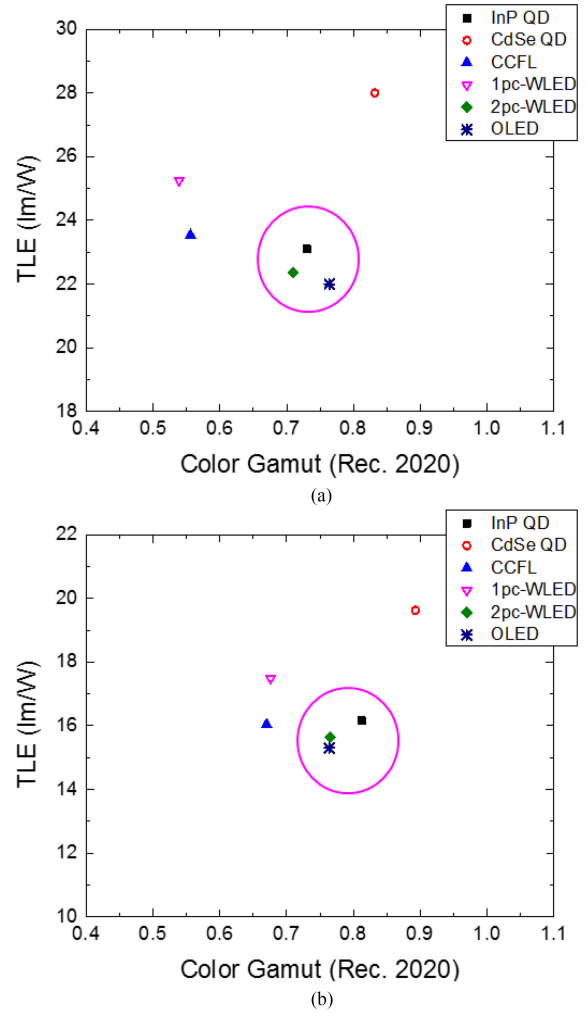


Fig. 12. TLE versus color gamut using (a) CF-1 and (b) CF-2. (Here, color gamut in CIE 1931 color space is employed).

[78], but its *TLE* is not representative because the definition for an emissive OLED’s light efficiency is totally different from a non-emissive LCD. From Fig. 12, the Cd-based QD-enhanced backlight shows the best performance in terms of light efficiency and color gamut. While 2pc-WLED, OLED, and InP QD hold a similar electro-optic performance. This is understandable because they all exhibit similar FWHM emission spectra (40 nm ~ 50 nm).

When comparing Fig. 12(a) with (b), we find an interesting phenomenon. Firstly, for all the backlight sources, the optical efficiency is drastically reduced when CF-2 color filters (i.e. narrower bandwidth but less efficient) are used. But for color gamut, the effect is reversed. For CCFL and 1pc-WLED, the improvement using narrower CF-2 is as large as 13% in Rec. 2020, but for 2pc-WLED and InP QD this improvement is only ~9%. For the CdSe QD, its color gamut only increases 6% in Rec. 2020, indicating that the backlight with purer emission peaks is less dependent on the color filters. Therefore, QD backlight would allow the use of broader band CFs (CF-1) for achieving balanced efficiency and color gamut.

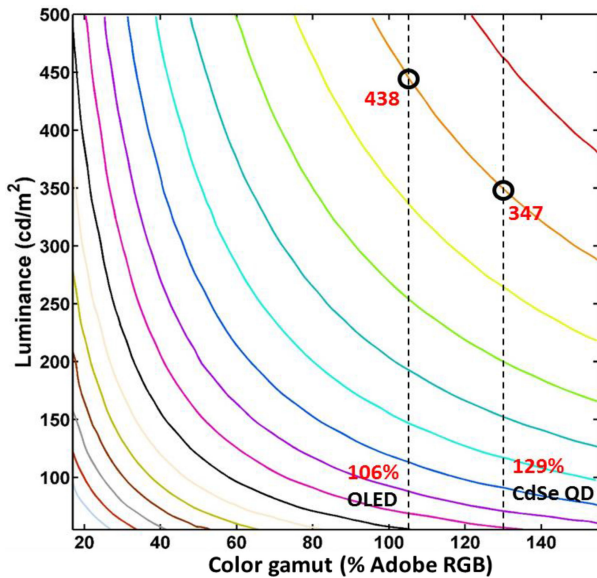


Fig. 13. Isoquality curves of the perceived quality metric (or known as display quality score).

C. Helmholtz–Kohlrausch Effect

Wide color gamut not only helps produce vivid colors but also helps reduce power consumption. This is due to the so-called Helmholtz–Kohlrausch (H-K) effect, in which a display with more saturated color is perceived to be brighter [79]–[82]. It is an entoptic phenomenon. As Fig. 13 depicts, the perceived quality metric (PQM) [83], or known as display quality score (DQS) [84], is proposed to describe the display quality quantitatively. This figure describes how display quality is affected by both luminance and color gamut. In this isoquality figure, the line at the upper right corner represents better perceived quality, and points on the same line is considered as equal quality. These lines are achieved using Adobe RGB in CIE 1976 color space.

Using the backlight sources described above, we could easily mark their points in this PQM (or DQS) figure. Here, we focus on the CdSe QD and OLED’s performances; the 2pc-WLED and InP QD exhibit similar color gamut as OLED. In comparison, CdSe QD shows much larger color gamut than OLED (129% vs. 106% Adobe RGE). When it comes to the perceived image quality, QD-LCD would be 1.26X more efficient than OLED (347 cd/m² vs. 438 cd/m²). Similar phenomenon has been reported when comparing OLED with 1pc-WLED based LCD [85], or in LED projectors [86], [87]. Fig. 14 illustrates this effect more clearly. For the same luminance intensity (347 cd/m²) [Fig. 14(a)], QD-LCD looks better than OLED due to its more saturated colors. To possess similar quality, we need to raise the luminance intensity of an OLED to 438 cd/m² [Fig. 14(b)].

V. FUTURE TRENDS

Because QD-enhanced backlight offers more saturated colors, and higher optical efficiency than conventional WLED, it has been widely used in high-end TVs, monitors, and pads. Lately, some advanced QD-based technologies are being actively inves-

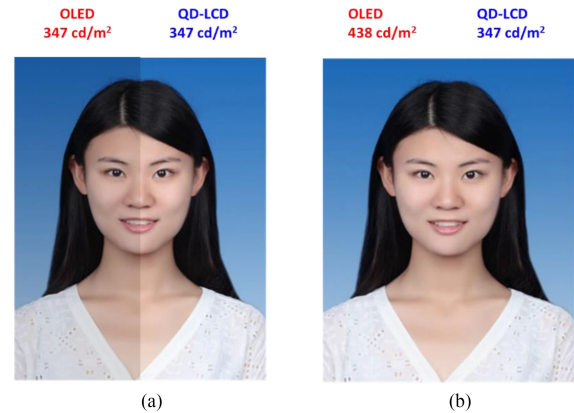


Fig. 14. Illustration of perceived image quality for OLED and QD-LCD.

tigated. Here we only highlight two of them, and discuss their inherent advantages, issues and potential solutions.

A. Quantum Dot Array for Color Filters

In conventional LCD panels, over 2/3 of the incident backlight is absorbed by the color filters (CFs) [75]. Thus, to improve optical efficiency, one approach is to remove or replace CFs. As an excellent energy down-conversion material, QD holds this promise. Fig. 15(a) depicts the proposed structure, where a patterned QD array is placed above the LC layer. A UV-LED or blue LED array is employed as the pumping source to excite the RGB QDs. Since there is no spatial CFs, the light efficiency should be tripled. Another implicit advantage is faster response time. This is because only blue light traverses through the LC layer, we can use a thinner cell gap to achieve the required phase retardation. A thinner LC cell leads to a faster response time. Meanwhile, viewing angle is greatly widened, owing to the isotropic emission of QDs. In 2016, Chen *et al.* combined QD array with a TN LC panel to achieve excellent performance, such as fast response time ($\tau_{\text{on}} + \tau_{\text{off}} < 3$ ms), wide viewing angle, and increased optical efficiency [88]. In their design, a deep blue LED with $\lambda = 410$ nm was employed to excite the RGB QD array.

The design concept of patterned QD array is intriguing, but some technical issues remain to be overcome. First, the backward emission of QD array should be recycled, otherwise half of the emitted light would be lost. A band-pass reflector provides a possible solution [Fig. 15(b)] as it transmits blue light, while reflecting green and red. This way, all the QD emissions can be fully utilized [89]. Such design is particularly attractive for virtual reality (VR) displays. In an immersed environment, there is no ambient light to excite the QD array.

If the display is exposed to an ambient light, then another serious concern would arise. Besides blue backlight, green and red QDs could be excited by the short-wavelength ambient light as well. As a result, the ambient contrast ratio would degrade substantially. To prevent this from happening, we can place a conventional color filter array above the QD layer to block the unwanted ambient light, as shown in Fig. 15(c) [89]. Let us examine the red pixels first. Under such condition, the red CFs

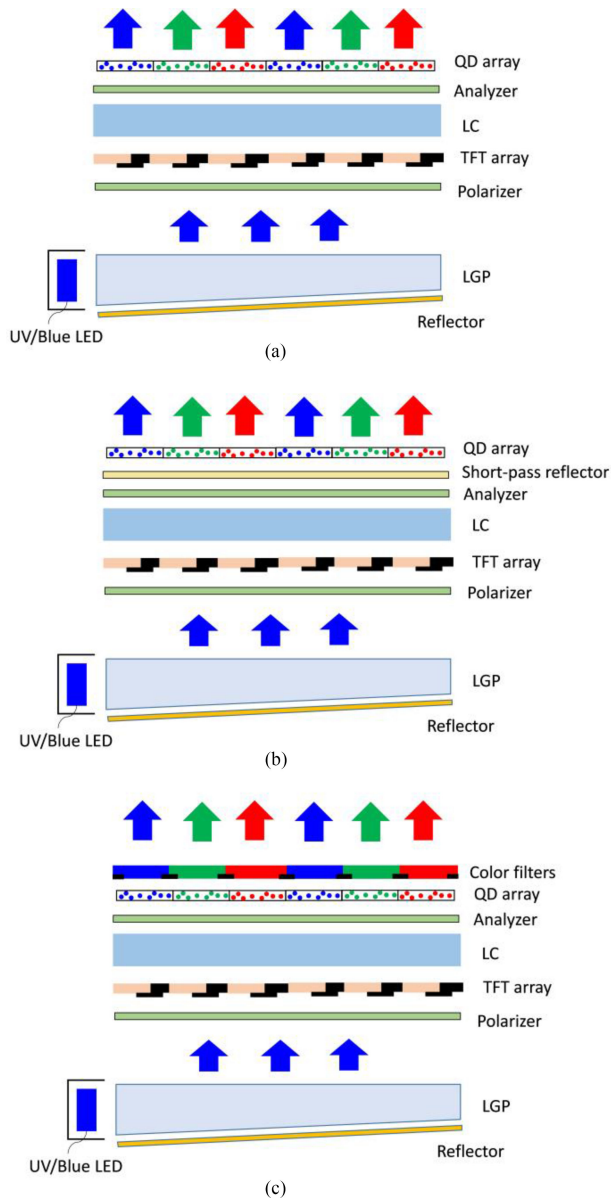


Fig. 15. Schematic diagram for three different configurations with patterned QD array. (a) Basic structure; (b) A short-pass reflector is placed below QD array to recycle backward emission; and (c) Conventional color filter is placed above QD array to prevent unwanted ambient light excitation.

only transmit the red ambient light, while blocking the green and blue contents of the ambient light. Similar principle applies to green and blue sub-pixels, too. However, the ambient light issue cannot be completely eliminated. The following two reasons may account for this imperfection: 1) QD materials exhibit self-absorption, which is very challenging to overcome [66]. 2) Conventional CFs exhibit relatively broad transmission band, so that there would be still some leakage from ambient light to excite the QD array. Fig. 16 illustrates this effect, where the blue shaded area represents the self-absorption of QD and light leakage induced by the color filter, which would degrade the ambient contrast ratio. Two possible solutions can be considered: 1) reducing the self-absorption by separating the absorption and emission spectra [66], [90]; 2) using a color filtering

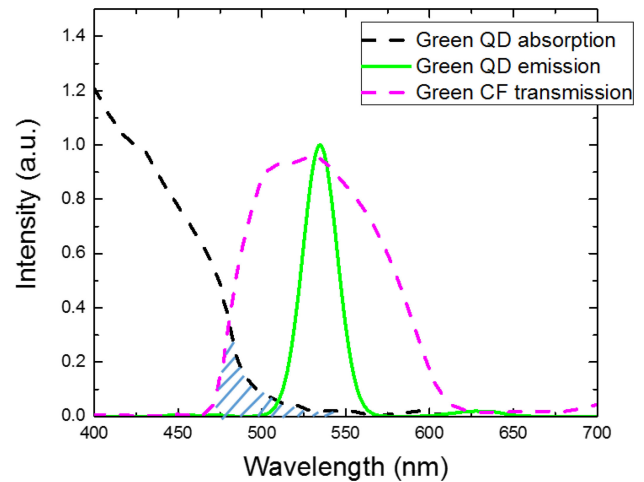


Fig. 16. Schematic diagram of light leakage and self-absorption of QDs.

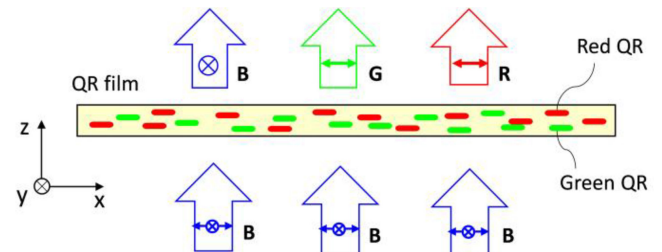


Fig. 17. Schematic diagram for an aligned QR film excited by unpolarized blue light.

material with steeper absorption edge, like J-aggregate mixture [91]–[98]. The latter has a sharp absorption edge [99], which would cut off the unwanted ambient light more efficiently.

B. Quantum Rod (QR)-Enhanced Backlight

The QD emission is isotropic and unpolarized, so that over 50% of the emitted light would be absorbed by the linear polarizer before entering the LC layer. To improve optical efficiency, quantum rod (QR) offers a viable option because the emitted light is partially linearly polarized [100]–[105]. When coupling into an LCD backlight, the transmittance through the polarizer is increased. The degree of improvement depends on the polarization ratio [106]. However, the challenge is how to align these QR nanoparticles in high quality [107]. Several approaches have been proposed, like electric field induced alignment [108], [109], magnetic field induced alignment [110], nanofiber induced alignment [111]–[113], liquid crystal induced alignment [114], mechanical rubbing induced alignment [115], etc. Until now, the nanofiber approach, where QRs are embedded in a well-aligned polymer nanofiber sheet, seems to be more favorable. Qlight Nanotech has released their QR-film prototype using such technique, called active brightness enhancement film (ABEF) [116]. Its polarization ratio reaches ~ 0.6 , leading to 20% improvement on the LCD light efficiency [113], [116].

Although the anisotropic emission of QR is desirable, one serious drawback is often overlooked, which is anisotropic absorption [117], [118]. As shown in Fig. 17, the unpolarized blue

light excites well-aligned green and red QRs. As expected, a partially linearly polarized green/red light is generated. Here we assume the larger dipole moment of QR nanoparticle is aligned in x-axis, which determines the preferred emission direction. But at the same time, the absorption along x-axis would be also much stronger than that of y-axis, leading to partially linearly polarized blue light. The polarization direction of the outgoing blue light is orthogonal to that of emitted green/red beams. In this case, a linear polarizer could easily deteriorate the color balance by absorbing either blue or green/red light. This polarization mismatch problem should be solved before QR-enhanced backlight can find widespread applications.

VI. CONCLUSION

We have briefly reviewed the recent progress of QD-enhanced LCDs. From material viewpoint, Cd-based QDs show the best performance, including narrow FWHM (~ 25 nm), high quantum efficiency ($>95\%$) and long-term stability ($>30,000$ hours). Meanwhile, heavy metal-free QDs are emerging: InP QDs are catching up in lifetime and quantum efficiency, but its FWHM needs further improvement. Regarding the device configuration, QDEF and QD rail have been commercialized, while the on-chip approach is still awaiting for the lifetime and compliant packaging issues to be resolved. As for the system level, we first investigate the effect of Gaussian fitting in the color gamut calculations, and observe a noticeable difference. Compared to other backlight sources, QD technology exhibits superior performance, like higher efficiency and wider color gamut. When considering the H-K effect, QD-enhanced LCD is 1.26X more efficient than OLED due to the more saturated primary colors. New trends for QD-LCDs are also highlighted. One is to use QD array to replace conventional color filters. Some specific structure designs are needed in order to utilize the backward emission and prevent ambient light excitation. Another one is quantum rod anisotropic backlight. It exhibits anisotropic emission, but also anisotropic absorption. The latter causes polarization mismatch between the transmitted blue light and the photoluminescent green/red light. The development of QD-LCD is still undergoing very actively. We believe the prime time for QD-enhanced LCDs is around the corner.

ACKNOWLEDGMENT

The authors would like to thank R. Zhu and G. Tan for helpful discussions, Y. Huang for providing her photograph, and Dr. Y.-T. Lu of EFUN Technology (Taiwan) for providing the QDEF sample shown in Fig. 6(b).

REFERENCES

- [1] S. Kobayashi, S. Mikoshiba, and S. Lim, *LCD Backlights*. New York, NY, USA: Wiley, 2009.
- [2] T. Okumura, A. Tagaya, Y. Koike, M. Horiguchi, and H. Suzuki, "Highly-efficient backlight for liquid crystal display having no optical films," *Appl. Phys. Lett.*, vol. 83, pp. 2515–2517, 2003.
- [3] K. Kälántár, "Modified functional light-guide plate for backlighting transmissive LCDs," *J. Soc. Inf. Display*, vol. 11, pp. 641–645, 2003.
- [4] D. Feng, Y. Yan, X. Yang, G. Jin, and S. Fan, "Novel integrated light-guide plates for liquid crystal display backlight," *J. Opt. A, Pure Appl. Opt.*, vol. 7, pp. 111–117, 2005.

- [5] M. Anandam, "Progress of LED backlights for LCDs," *J. Soc. Inf. Display*, vol. 16, pp. 287–310, 2008.
- [6] H. T. Huang, Y. P. Huang, and C. C. Tsai, "Planar lighting system using array of blue LEDs to excite yellow remote phosphor film," *J. Display Technol.*, vol. 7, pp. 44–51, 2011.
- [7] "Parameter values for the HDTV standards for production and international programme Exchange," ITU Recommendation BT.709-6, 2015.
- [8] "Parameter values for ultra-high definition television systems for production and international programme exchange," ITU Recommendation BT.2020-2, 2015.
- [9] K. Masaoka, Y. Nishida, M. Sugawara, and E. Nakasu, "Design of primaries for a wide-gamut television colorimetry," *IEEE Trans. Broadcast.*, vol. 56, no. 4, pp. 452–457, Dec. 2010.
- [10] G. Harbers and C. Hoelen, "High performance LCD backlighting using high intensity red, green and blue light emitting diodes," in *Proc. SID Symp. Dig. Tech. Papers*, 2001, vol. 32, pp. 702–705.
- [11] R. S. West *et al.*, "High brightness direct LED backlight for LCD TV," in *Proc. SID Symp. Dig. Tech. Papers*, 2003, vol. 34, pp. 1262–1265.
- [12] W. Folkerts, "LED backlighting concepts with high flux LEDs," in *Proc. SID Symp. Dig. Tech. Papers*, 2004, vol. 35, pp. 1226–1229.
- [13] R. B. Lu, S. Gauza, and S. T. Wu, "LED-lit LCD TVs," *Mol. Cryst. Liq. Cryst.*, vol. 488, pp. 246–259, 2008.
- [14] H. J. Chiu and S. J. Cheng, "LED backlight driving system for large-scale LCD panels," *IEEE Trans. Ind. Electron.*, vol. 54, no. 5, pp. 2751–2760, Oct. 2007.
- [15] C. Y. Wu, T. F. Wu, J. R. Tsai, Y. M. Chen, and C. C. Chen, "Multistring LED backlight driving system for LCD panels with color sequential display and area control," *IEEE Trans. Ind. Electron.*, vol. 55, no. 10, pp. 3791–3800, Oct. 2008.
- [16] E. F. Schubert, T. Gessmann, and J. K. Kim, *Light Emitting Diodes*. New York, NY, USA: Wiley, 2005.
- [17] R. J. Xie, N. Hirosaki, and T. Takeda, "Wide color gamut backlight for liquid crystal displays using three-band phosphor-converted white light-emitting diodes," *Appl. Phys. Express*, vol. 2, 2009, Art. no. 022401.
- [18] Y. Ito, T. Hori, T. Kusunoki, H. Nomura, and H. Kondo, "A phosphor sheet and a backlight system providing wider color gamut for LCDs," *J. Soc. Inf. Display*, vol. 22, pp. 419–428, 2014.
- [19] J. H. Oh, H. Kang, M. Ko, and Y. R. Do, "Analysis of wide color gamut of green/red bilayered freestanding phosphor film-capped white LEDs for LCD backlight," *Opt. Express*, vol. 23, pp. A791–A804, 2015.
- [20] L. Wang *et al.*, "Highly efficient narrow-band green and red phosphors enabling wider color-gamut LED backlight for more brilliant displays," *Opt. Express*, vol. 23, pp. 28707–28717, 2015.
- [21] N. Hirosaki *et al.*, "Characterization and properties of green-emitting β -SiAlON:Eu²⁺ powder phosphors for white light-emitting diodes," *Appl. Phys. Lett.*, vol. 86, 2009, Art. no. 211905.
- [22] R. J. Xie, N. Hirosaki, H. L. Li, Y. Q. Li, and M. Mitomo, "Synthesis and photoluminescence properties of β -sialon:Eu²⁺ (Si₆-zAlzOzN₈-z:Eu²⁺) - A promising green oxynitride phosphor for white light-emitting diodes," *J. Electrochem. Soc.*, vol. 154, pp. J314–J319, 2008.
- [23] S. Adachi and T. Takahashi, "Direct synthesis and properties of K₂SiF₆:Mn⁴⁺ phosphor by wet chemical etching of Si wafer," *J. Appl. Phys.*, vol. 104, 2008, Art. no. 023512.
- [24] T. Takahashi and S. Adachi, "Synthesis of K₂SiF₆:Mn⁴⁺ red phosphor from silica glasses by wet chemical etching in HF/KMnO₄ solution," *Electrochem. Solid State Lett.*, vol. 12, pp. J69–J71, 2009.
- [25] J. E. Murphy, F. Garcia-Santamaria, A. A. Setlur, and S. Sista, "PFS, K₂SiF₆:Mn⁴⁺: The red-line emitting LED phosphor behind GE's Tri-Gain Technology™ platform," in *Proc. SID Symp. Dig. Tech. Papers*, 2015, vol. 46, pp. 927–930.
- [26] E. Jang *et al.*, "White-light-emitting diodes with quantum dot color converters for display backlights," *Adv. Mater.*, vol. 22, pp. 3076–3080, 2010.
- [27] Z. Luo, Y. Chen, and S. T. Wu, "Wide color gamut LCD with a quantum dot backlight," *Opt. Express*, vol. 21, pp. 26269–26284, 2013.
- [28] S. Coe-Sullivan, W. Liu, P. Allen, and J. S. Steckel, "Quantum dots for LED downconversion in display applications," *ECS J. Solid State Sci. Technol.*, vol. 2, pp. R3026–R3030, 2013.
- [29] Y. Shirasaki, G. J. Supran, M. G. Bawendi, and V. Bulović, "Emergence of colloidal quantum-dot light-emitting technologies," *Nat. Photon.*, vol. 7, pp. 13–23, 2013.
- [30] J. S. Steckel *et al.*, "Quantum dot manufacturing requirements for the high volume LCD market," in *Proc. SID Symp. Dig. Tech. Papers*, 2013, vol. 44, pp. 943–945.
- [31] Z. Luo, D. Xu, and S. T. Wu, "Emerging quantum-dots-enhanced LCDs," *J. Display Technol.*, vol. 10, pp. 526–539, 2014.

- [32] K. Bourzac, "Quantum dots go on display," *Nature*, vol. 493, p. 283, 2013.
- [33] J. S. Steckel *et al.*, "Quantum dots: The ultimate down-conversion material for LCD displays," *J. Soc. Inf. Display*, vol. 23, pp. 294–305, 2015.
- [34] Q. Hong, K. C. Lee, Z. Luo, and S. T. Wu, "High-efficiency quantum dot remote phosphor film," *Appl. Opt.* vol. 54, pp. 4617–4622, 2015.
- [35] L. Goldstein, F. Glas, J. Y. Marzin, M. N. Charasse, and G. Le Roux, "Growth by molecular beam epitaxy and characterization of InAs/GaAs strained-layer superlattices," *Appl. Phys. Lett.*, vol. 47, pp. 1099–1101, 1985.
- [36] C. Murray, D. J. Norris, and M. G. Bawendi, "Synthesis and characterization of nearly monodisperse CdE (E = sulfur, selenium, tellurium) semiconductor nanocrystallites," *J. Amer. Chem. Soc.*, vol. 115, pp. 8706–8715, 1993.
- [37] M. A. Hines and P. Guyot-Sionnest, "Synthesis and characterization of strongly luminescing ZnS-capped CdSe nanocrystals," *J. Phys. Chem.*, vol. 100, pp. 468–471, 1996.
- [38] B. O. Dabbousi *et al.*, "(CdSe) ZnS core-shell quantum dots: Synthesis and characterization of a size series of highly luminescent nanocrystallites," *J. Phys. Chem. B*, vol. 101, pp. 9463–9475, 1997.
- [39] M. Bruchez, M. Moronne, P. Gin, S. Weiss, and A. P. Alivisatos, "Semiconductor nanocrystals as fluorescent biological labels," *Science*, vol. 281, pp. 2013–2016, 1998.
- [40] Y. Yin and A. P. Alivisatos, "Colloidal nanocrystal synthesis and the organic-inorganic interface," *Nature*, vol. 437, pp. 664–670, 2005.
- [41] A. M. Smith and S. M. Nie, "Semiconductor nanocrystals: Structure, properties, and band gap engineering," *Acc. Chem. Res.*, vol. 43, pp. 190–200, 2010.
- [42] L. Brus, "Electronic wave-functions in semiconductor clusters—Experiment and theory," *J. Phys. Chem.*, vol. 90, pp. 2555–2560, 1986.
- [43] S. Ithurria and B. Dubertret, "Quasi 2D colloidal CdSe platelets with thicknesses controlled at the atomic level," *J. Amer. Chem. Soc.*, vol. 130, pp. 16504–16505, 2008.
- [44] S. Ithurria, G. Bousquet, and B. Dubertret, "Continuous transition from 3D to 1D confinement observed during the formation of CdSe nanoplatelets," *J. Amer. Chem. Soc.*, vol. 133, pp. 3070–3077, 2011.
- [45] B. O. Dabbousi, M. G. Bawendi, O. Onitsuka, and M. F. Rubner, "Electroluminescence from CdSe quantum-dot/polymer composites," *Appl. Phys. Lett.*, vol. 66, pp. 1316–1318, 1995.
- [46] P. Reiss, M. Potiere, and L. Li, "Core/shell semiconductor nanocrystals," *Small*, vol. 5, pp. 154–168, 2009.
- [47] M. Green, "The nature of quantum dot capping ligands," *J. Mater. Chem.*, vol. 20, pp. 5797–5809, 2010.
- [48] M. J. Anc, N. L. Pickett, N. C. Gresty, J. A. Harris, and K. C. Mishra, "Progress in non-Cd quantum dot development for lighting applications," *J. Solid State Sci. Technol.*, vol. 2, pp. R3071–R3082, 2013.
- [49] X. Y. Yang *et al.*, "Full visible range covering InP/ZnS nanocrystals with high photometric performance and their application to white quantum dot light-emitting diodes," *Adv. Mater.*, vol. 24, pp. 4180–4185, 2012.
- [50] H. Kim *et al.*, "Characteristics of CuInS₂/ZnS quantum dots and its application on LED," *J. Cryst. Growth*, vol. 326, pp. 90–93, 2011.
- [51] H. Menkara *et al.*, "Development of nanophosphors for light emitting diodes," *Opt. Express*, vol. 19, pp. A972–A981, 2011.
- [52] P. O. Anikeeva, J. E. Halpert, M. G. Bawendi, and V. Bulovic, "Quantum dot light-emitting devices with electroluminescence tunable over the entire visible spectrum," *Nano Lett.*, vol. 9, pp. 2532–2536, 2009.
- [53] J. Thielen, J. Hillis, J. Van Derlofske, D. Lamb, and A. Lathrop, "Quantum dots and Rec. 2020: Bringing the color of tomorrow closer to reality today," *SMPTE Motion Imag. J.*, vol. 124, pp. 19–25, 2015.
- [54] R. Zhu, Z. Luo, H. Chen, Y. Dong, and S. T. Wu, "Realizing Rec. 2020 color gamut with quantum dot displays," *Opt. Express*, vol. 23, pp. 23680–23693, 2015.
- [55] "Restriction of the Use of Certain Hazardous Substances in Electrical and Electronic Equipment," EU Directive 2002/95/EC, 2003.
- [56] N. L. Pickett, N. C. Gresty, and M. A. Hines, "Heavy metal-free quantum dots making inroads for consumer applications," in *Proc. SID Symp. Dig. Tech. Papers*, 2016, vol. 47, pp. 425–427.
- [57] X. Yang *et al.*, "A bright cadmium-free, hybrid organic/quantum dot white light-emitting diode," *Appl. Phys. Lett.* vol. 101, 2012, Art. no. 233110.
- [58] J. Lim *et al.*, "Highly efficient cadmium-free quantum dot light-emitting diodes enabled by the direct formation of excitons within InP@ZnSe quantum dots," *ACS Nano*, vol. 7, pp. 9019–9026, 2013.
- [59] Y. Kim *et al.*, "Indium phosphide-based colloidal quantum dot light emitting diodes on flexible substrate," *Nanosci. Nanotechnol. Lett.* vol. 5, pp. 1065–1069, 2013.
- [60] S. H. Lee *et al.*, "Remote-type, high-color gamut white light-emitting diode based on InP quantum dot color converters," *Opt. Mater. Express*, vol. 4, pp. 1297–1302, 2014.
- [61] S. J. Yang, J. H. Oh, S. Kim, H. Yang, and Y. R. Do, "Realization of InP/ZnS quantum dots for green, amber and red down-converted LEDs and their color-tunable, four-package white LEDs," *J. Mater. Chem. C*, vol. 3, pp. 3582–3591, 2015.
- [62] C. Ippen *et al.*, "Color tuning of indium phosphide quantum dots for cadmium-free quantum dot light-emitting devices with high efficiency and color saturation," *J. Soc. Inf. Display*, vol. 23, pp. 285–293, 2015.
- [63] N. L. Pickett, J. A. Harris, and N. C. Gresty, "Heavy metal-free quantum dots for display applications," in *Proc. SID Symp. Dig. Tech. Papers*, 2015, vol. 46, pp. 168–169.
- [64] E. Lee *et al.*, "Greener quantum-dot enabled LCDs with BT. 2020 color gamut," in *Proc. SID Symp. Dig. Tech. Papers*, 2016, vol. 47, pp. 549–551.
- [65] S. Sadasivan, K. Bausemer, S. Corliss, and R. Pratt, "Performance benchmarking of wide color gamut televisions and monitors," in *Proc. SID Symp. Dig. Tech. Papers*, 2016, vol. 47, pp. 333–335.
- [66] J. Kurtin, N. Puetz, B. Theobald, N. Stott, and J. Osinski, "Quantum dots for high color gamut LCD displays using an on-chip LED solution," in *Proc. SID Symp. Dig. Tech. Papers*, 2014, vol. 45, pp. 146–148.
- [67] Y. Zhao *et al.*, "High-temperature luminescence quenching of colloidal quantum dots," *ACS Nano*, vol. 6, pp. 9058–9067, 2015.
- [68] W. Chen *et al.*, "Luminescent nanocrystals and composites for high quality displays and lighting," in *Proc. SID Symp. Dig. Tech. Papers*, 2016, vol. 47, pp. 556–559.
- [69] S. Coe-Sullivan, "The quantum dot revolution: Marching towards the mainstream," in *Proc. SID Symp. Dig. Tech. Papers*, 2016, vol. 47, pp. 239–240.
- [70] K. Twietmeyer and S. Sadasivan, "Design considerations for highly efficient edge-lit quantum dot displays," *J. Soc. Inf. Display*, vol. 24, pp. 312–322, 2016.
- [71] J. Chen, V. Hardev, J. Hartlove, J. Hofler, and E. Lee, "A high-efficiency wide-color-gamut solid-state backlight system for LCDs using quantum dot enhancement film," in *Proc. SID Symp. Dig. Tech. Papers*, 2012, vol. 43, pp. 895–896.
- [72] J. Thielen *et al.*, "Correlation of accelerated aging to in-device lifetime of quantum dot enhancement film," in *Proc. SID Symp. Dig. Tech. Papers*, 2016, vol. 47, pp. 336–339.
- [73] J. Chen, V. Hardev, and J. Yurek, "Quantum dot displays: Giving LCDs a competitive edge through color," *Inf. Display*, vol. 1, pp. 2–7, 2013.
- [74] J. V. Derlofske *et al.*, "Quantum dot enhancement film (QDEF)," 3M White Paper, 2013. [Online]. Available: <http://multimedia.3m.com/mws/media/9853750/3mtm-quantum-dot-enhancement-film-qdef-white-paper.pdf?fn=Quantum%20Dot%20QDEF%20Whitepaper.pdf>
- [75] D. K. Yang and S. T. Wu, *Fundamentals of Liquid Crystal Devices*, 2nd ed. New York, NY, USA: Wiley, 2014.
- [76] G. Wyszecki and W. Stiles, *Color Science—Concepts and Methods, Quantitative Data and Formulate*, 2nd ed. New York, NY, USA: Wiley, 1982.
- [77] R. Lu, Q. Hong, S. T. Wu, K. H. Peng, and H. S. Hsieh, "Quantitative comparison of color performances between IPS and MVA LCDs," *J. Display Technol.*, vol. 2, pp. 319–326, 2006.
- [78] J. P. Spindler and T. K. Hatwar, "Development of tandem white architecture for large-sized AMOLED displays with wide color gamut," in *Proc. SID Symp. Dig. Tech. Papers*, 2007, vol. 38, pp. 89–92.
- [79] Y. Nayatani, "Simple estimation methods for the Helmholtz-Kohlrausch effect," *Color Res. Appl.*, vol. 22, pp. 385–401, 1997.
- [80] R. L. Donofrio, "The Helmholtz-Kohlrausch effect," *J. Soc. Inf. Display*, vol. 19, pp. 658–664, 2011.
- [81] T. Shizume, G. Ohashi, H. Takamatsu, and Y. Shimodaira, "Estimation of the Helmholtz–Kohlrausch effect for natural images," *J. Soc. Inf. Display*, vol. 22, pp. 588–596, 2014.
- [82] J. F. Van Derlofske *et al.*, "Illuminating the value of larger color gamut for quantum dot displays," in *Proc. SID Symp. Dig. Tech. Papers*, 2014, vol. 45, pp. 237–240.
- [83] J. F. Schumacher, J. V. Derlofske, B. Stankiewicz, D. Lamb, and Art Lathrop, "PQM: A new quantitative tool for evaluating display design options," 3M Optical Systems Division, 2014. [Online]. Available: http://solutions.3m.com/3MContentRetrievalAPI/BlobServlet?lmd=1371108782000&locale=en_WW&assetType=MMM_Image&assetId=1361624032435&blobAttribute=ImageFile
- [84] J. F. Schumacher *et al.*, "3MDQS 1.0: A new quantitative tool for evaluating display design options," 3M White Paper, 2014. [Online]. Available: <http://multimedia.3m.com/mws/media/9773370/3m-display-quality->

- score-1-0-a-new-quantitative-tool.pdf?fn=Display%20Quality%20Score%20Whitepaper
- [85] T. Tsujimura *et al.*, "Advancements and outlook of high performance active-matrix OLED displays," in *Proc. SID Symp. Dig. Tech. Papers*, 2007, vol. 38, pp. 84–88.
- [86] S. F. Liao, H. Y. Chou, T. H. Yang, C. C. Lee, and K. Chang, "Perceived brightness of LED projector," in *Proc. SID Symp. Dig. Tech. Papers*, 2009, vol. 40, pp. 262–264.
- [87] S. F. Liao, T. H. Yang, C. C. Lee, K. Chang, and N. Chiu, "Color perception in LED projectors," in *Proc. SID Symp. Dig. Tech. Papers*, 2011, vol. 42, pp. 229–231.
- [88] J. P. Yang, E. L. Hsiang, and H. M. Philip Chen, "Wide viewing angle TN LCD enhanced by printed quantum-dots film," in *Proc. SID Symp. Dig. Tech. Papers*, 2016, vol. 47, pp. 21–24.
- [89] H. J. Kim, M. H. Shin, J. S. Kim, and Y. J. Kim, "Optical efficiency enhancement in wide color gamut LCD by a patterned quantum dot film and short pass reflector," in *Proc. SID Symp. Dig. Tech. Papers*, 2016, vol. 47, pp. 827–829.
- [90] L. Su, X. Zhang, Y. Zhang, and A. L. Rogach, "Recent progress in quantum dot based white light-emitting devices," *Top Current Chem.*, vol. 374, pp. 1–25, 2016.
- [91] H. Yao, "Morphology transformations in solutions: dynamic supramolecular aggregates," *Annu. Rep. Prog. Chem., Sect. C, Phys. Chem.*, vol. 100, pp. 99–148, 2004.
- [92] J. M. Chan, J. R. Tischler, S. E. Kooi, V. Bulovic, and T. M. Swager, "Synthesis of J-aggregating dibenz [a, j] anthracene-based macrocycles," *J. Amer. Chem. Soc.*, vol. 131, pp. 5659–5666, 2009.
- [93] F. Würthner, T. E. Kaiser, and C. R. Saha-Möller, "J-aggregates: from serendipitous discovery to supramolecular engineering of functional dye materials," *Angewandte Chemie- Int. Ed.*, vol. 50, pp. 3376–3410, 2011.
- [94] M. Sauer, J. Hofkens, and J. Enderlein, "Basic principles of fluorescence spectroscopy," in *Handbook of Fluorescence Spectroscopy and Imaging: From Single Molecules to Ensembles*. New York, NY, USA: Wiley, 2011, pp. 1–30.
- [95] C. Göll, M. Malkoç, S. Yeşilot, and M. Durmuş, "A first archetype of boron dipyrromethene-phthalocyanine pentad dye: design, synthesis, and photophysical and photochemical properties," *Dalton Trans.*, vol. 43, pp. 7561–7569, 2014.
- [96] J. F. Chang *et al.*, "Process dependence of morphology and microstructure of cyanine dye J-aggregate film: Correlation with absorption, photo- and electroluminescence properties," *Opt. Express*, vol. 22, pp. 29388–29397, 2014.
- [97] H. S. Wei *et al.*, "Adjustable exciton-photon coupling with giant Rabi-splitting using layer-by-layer J-aggregate thin films in all-metal mirror microcavities," *Opt. Express*, vol. 21, pp. 21365–21373, 2013.
- [98] Y. Qiao *et al.*, "Nanotubular J-aggregates and quantum dots coupled for efficient resonance excitation energy transfer," *ACS Nano*, vol. 9, pp. 1552–1560, 2015.
- [99] M. Sakamoto and M. Nagasawa, "Color correction filter, image display, and liquid crystal display," U.S. Patent 12/526,594, 2008.
- [100] X. Peng *et al.*, "Shape control of CdSe nanocrystals," *Nature*, vol. 404, pp. 59–61, 2000.
- [101] J. Hu *et al.*, "Linearly polarized emission from colloidal semiconductor quantum rods," *Science*, vol. 292, pp. 2060–2063, 2001.
- [102] Z. A. Peng and X. Peng, "Nearly monodisperse and shape-controlled CdSe nanocrystals via alternative routes: nucleation and growth," *J. Amer. Chem. Soc.*, vol. 124, pp. 3343–3353, 2002.
- [103] S. P. Ahrenkiel *et al.*, "Synthesis and characterization of colloidal InP quantum rods," *Nano Lett.*, vol. 3, pp. 833–837, 2003.
- [104] T. Mokari, E. Rothenberg, I. Popov, R. Costi, and U. Banin, "Selective growth of metal tips onto semiconductor quantum rods and tetrapods," *Science*, vol. 304, pp. 1787–1790, 2004.
- [105] F. Shieh, A. E. Saunders, and B. A. Korgel, "General shape control of colloidal CdS, CdSe, CdTe quantum rods and quantum rod heterostructures," *J. Phys. Chem. B*, vol. 109, pp. 8538–8542, 2005.
- [106] Z. Luo, Y. W. Cheng, and S. Y. Wu, "Polarization-preserving light guide plate for a linearly polarized backlight," *J. Display Technol.*, vol. 10, pp. 208–214, 2014.
- [107] M. Artemyev, B. Möller, and U. Woggon, "Unidirectional alignment of CdSe nanorods," *Nano Lett.*, vol. 3, pp. 509–512, 2003.
- [108] Z. Hu, M. D. Fischbein, C. Querner, and M. Drndic, "Electric-field-driven accumulation and alignment of CdSe and CdTe nanorods in nanoscale devices," *Nano Lett.*, vol. 6, pp. 2585–2591, 2006.
- [109] M. Mohammadimasoudi *et al.*, "Fast and versatile deposition of aligned semiconductor nanorods by dip-coating on a substrate with interdigitated electrodes," *Opt. Mater. Express*, vol. 3, pp. 2045–2054, 2013.
- [110] F. Pietra *et al.*, "Self-assembled CdSe/CdS nanorod sheets studied in the bulk suspension by magnetic alignment," *ACS Nano*, vol. 8, pp. 10486–10495, 2014.
- [111] T. Aubert *et al.*, "Large-scale and electroswitchable polarized emission from semiconductor nanorods aligned in polymeric nanofibers," *ACS Photon.*, vol. 2, pp. 583–588, 2015.
- [112] K. Wang, J. Qin, J. Hao, and W. Chen, "Large-scale brightness enhancement film with quantum rods aligned in polymeric nanofibers for high efficiency wide color gamut LED display," in *Proc. IEEE Photon. Conf.*, 2015, pp. 49–50.
- [113] M. Hasegawa, Y. Hirayama, and S. Dertinger, "Alignment of quantum rods," in *Proc. SID Symp. Dig. Tech. Papers*, 2015, vol. 46, pp. 67–70.
- [114] L. S. Li and A. P. Alivisatos, "Semiconductor nanorod liquid crystals and their assembly on a substrate," *Adv. Mater.*, vol. 15, pp. 408–411, 2003.
- [115] Y. Amit, A. Faust, I. Lieberman, L. Yedidya, and U. Banin, "Semiconductor nanorod layers aligned through mechanical rubbing," *Phys. Status Solidi A*, vol. 209, pp. 235–242, 2012.
- [116] E. Shaviv, D. Glozman, Y. Bonfil, U. Banin, and S. Amir, "Semiconductor quantum rods for display applications," in *Proc. SID Symp. Dig. Tech. Papers*, 2015, vol. 46, pp. 71–72.
- [117] X. Chen *et al.*, "Polarization spectroscopy of single CdSe quantum rods," *Phys. Rev. B*, vol. 64, 2001, Art. no. 245304.
- [118] J. S. Kamal *et al.*, "Direct determination of absorption anisotropy in colloidal quantum rods," *Phys. Rev. B*, vol. 85, 2012, Art. no. 035126.

Haiwei Chen received the B.S. degree in optoelectronic information engineering from Beihang University, Beijing, China, in 2013. He is currently working toward the Ph.D. degree in the College of Optics and Photonics, University of Central Florida, Orlando, FL, USA.

His research interests include wide color gamut, high dynamic range, and fast-response liquid crystal display devices. He has published 27 journal papers and 14 conference proceedings.

He received the SID Distinguished Student Paper Award in two consecutive years (2015 and 2016). He was the President of SID student chapter at University of Central Florida in 2016.

Juan He received the B.S. and M.S. degrees from the Department of Physics, Peking University, Beijing, China, in 2011 and 2014, respectively. She is currently working toward the Ph.D. degree in the College of Optics and Photonics, University of Central Florida (UCF), Orlando, FL, USA.

Her research focuses on quantum dots and other active materials for displays, sensing, and lasing applications. She has published 7 journal papers and 3 conference proceedings.

Ms. He received the SID Distinguished Student Paper Award in 2016. She is currently the President of the IEEE Photonics Society student chapter at UCF.

Shin-Tson Wu (M'98–SM'99–F'04) received the B.S. degree in physics from National Taiwan University, Taipei, Taiwan, and the Ph.D. degree from the University of Southern California, Los Angeles, CA, USA.

He is a Pegasus Professor with the College of Optics and Photonics, University of Central Florida, Orlando, FL, USA.

Dr. Wu is a Fellow of the Society of Information Display (SID), the Optical Society of America (OSA), and the SPIE. He is among the first six inductees of the Florida Inventors Hall of Fame (2014) and is a Charter Fellow of the National Academy of Inventors (2012). He received the OSA Esther Hoffman Beller Medal (2014), honorary Professor at Nanjing University (2013), the SID Slottow-Owaki prize (2011), the OSA Joseph Fraunhofer award (2010), the SPIE G. G. Stokes award (2008), and the SID Jan Rajchman prize (2008). He was the founding Editor-in-Chief of the IEEE/OSA JOURNAL OF DISPLAY TECHNOLOGY.